

# **Continental Patterns of Bird Migration Linked** to Climate Variability

Amin Dezfuli, Kyle G. Horton, Benjamin Zuckerberg, Siegfried D. Schubert, and Michael G. Bosilovich

> **ABSTRACT:** For ~100 years, the continental patterns of avian migration in North America have been described in the context of three or four primary flyways. This spatial compartmentalization often fails to adequately reflect a critical characterization of migration—phenology. This shortcoming has been partly due to the lack of reliable continental-scale data, a gap filled by our current study. Here, we leveraged unique radar-based data quantifying migration phenology and used an objective regionalization approach to introduce a new spatial framework that reflects interannual variability. Therefore, the resulting spatial classification is intrinsically different from the "flyway concept." We identified two regions with distinct interannual variability of spring migration across the contiguous United States. This data-driven framework enabled us to explore the climatic cues affecting the interannual variability of migration phenology, "specific to each region" across North America. For example, our "two-region" approach allowed us to identify an east-west dipole pattern in migratory behavior linked to atmospheric Rossby waves. Also, we revealed that migration movements over the western United States were inversely related to interannual and low-frequency variability of regional temperature. A similar link, but weaker and only for interannual variability, was evident for the eastern region. However, this region was more strongly tied to climate teleconnections, particularly to the east Pacific-North Pacific (EP-NP) pattern. The results suggest that oceanic forcing in the tropical Pacific—through a chain of processes including Rossby wave trains—controls the climatic conditions, associated with bird migration over the eastern United States. Our spatial platform would facilitate better understanding of the mechanisms responsible for broadscale migration phenology and its potential future changes.

> **KEYWORDS:** Atmosphere; Ecology; North America; Rossby waves; Interannual variability; Animal studies

https://doi.org/10.1175/BAMS-D-21-0220.1

Corresponding author: Amin Dezfuli, amin.dezfuli@nasa.gov

In final form 18 November 2021

©2022 American Meteorological Society

For information regarding reuse of this content and general copyright information, consult the AMS Copyright Policy.

AFFILIATIONS: Dezfuli and Schubert—Global Modeling and Assimilation Office, NASA Goddard Space Flight Center, Greenbelt, and Science Systems and Applications, Inc., Lanham, Maryland; Horton—Department of Fish, Wildlife, and Conservation Biology, Colorado State University, Fort Collins, Colorado; Zuckerberg—Department of Forest and Wildlife Ecology, University of Wisconsin–Madison, Madison, Wisconsin; Bosilovich—Global Modeling and Assimilation Office, NASA Goddard Space Flight Center, Greenbelt, Maryland

he seasonal migration of birds is a prominent feature of the natural world. Every spring, migratory birds arrive from south and central America to the contiguous United States (CONUS) and Canada for breeding (Gauthreaux 1971; Lowery 1945; Dokter et al. 2018; Lane et al. 2012). Exogenous forces, such as climate and changes in primary productivity, influence migration speed and phenology, defined as the seasonal timing of life cycle events (La Sorte et al. 2014a; Zuckerberg et al. 2020; Gordo 2007; Smith and Deppe 2008). Endogenous forces, such as circadian cycles and site fidelity, also play a role (Gwinner 1996; Cohen et al. 2012; Alerstam et al. 2003). Together, these forces suggest that migratory pathways should be stable over time, but also reflect broadscale and regular patterns in climate variability. Traditionally, spatial classification of bird migration in CONUS is viewed in the context of "flyways," and the region is commonly divided into four principal routes (Pacific, Central, Mississippi, and Atlantic), largely derived from waterfowl ecology (Hawkins 1984; Lincoln 1935; Waller et al. 2018). An alternative representation is three routes, western, central, and eastern (La Sorte et al. 2014b; Horton et al. 2020), although some similarities have been identified between the latter two routes that may be indicative of a larger migration system (La Sorte et al. 2014b).

However, such a large-scale characterization of migratory routes has not been fully understood, and the common spatial classification approaches are either subjective or based on the time-averaged migratory behavior and therefore neglect year-to-year variability (Hawkins 1984; La Sorte et al. 2014b; Olsen et al. 2006). Those studies that consider interannual variability are limited to observations from individual sites (Van Buskirk et al. 2009; Oliver et al. 2020; Ballard et al. 2003). To fill these voids, we have proposed a new geographic framework, which would reflect the interannual variability of bird migration at the continental scale. This approach would be essential for better understanding how patterns in climate variability influence broadscale animal movements and migration phenology (Strong et al. 2015; Zuckerberg et al. 2020).

The main obstacle for spatiotemporal analysis of bird migration has been the lack of reliable data over a sufficiently long period and with broad spatial coverage across CONUS (Horton et al. 2020). This data limitation has hampered the proper assessments of spatial properties and annual timing events. Recently published data of migration phenology, derived from weather radar observations (Horton et al. 2020), provides a unique opportunity to perform such analysis at the continental scale. Leveraging these data, we have revisited the traditional spatial framework to test whether there is coherent interannual and low-frequency variability in migration timing across the continent, and whether that exhibits spatial variability that could be used to improve our knowledge of the drivers of year-to-year variability of bird migration. In other words, we aim to identify subregions based on similarity of interannual variability of bird migration and consequently explore regional and remote climatic drivers specific to each region.

### **Bird migration data**

We used nocturnal migration data that have been recently compiled from the NOAA's Next Generation Radar (NEXRAD) system (Horton et al. 2020). NEXRAD is a network of 143 stations across the contiguous United States and provides exceptional spatial and temporal coverage for continental-scale analysis (Ansari et al. 2018; Dokter et al. 2019; Rosenberg et al. 2019). Real-time and archived NEXRAD data are shared on Amazon Web Service (AWS) and can be accessed via simple application program interfaces (APIs). The AWS cloud has facilitated data access and created new research opportunities, including analysis of avian migration.

The bird migration data have been developed using a convolutional neural network (CNN) to exclude precipitation contamination and subsequently quantify the phenology of migratory movements (Lin et al. 2019). This approach employs a neural network trained using per-pixel labels (biology or weather) derived from a polarimetric variable, specifically correlation coefficient ( $\rho_{\rm HV}$ ). Correlation coefficient quantifies the consistency of the shapes and sizes of targets within the radar beam and is used to distinguish between meteorological and non-meteorological objects. If the correlation coefficient exceeds 0.95, reflectivity is classified as precipitation, otherwise it is classified as biological. Their algorithm also removes stationary clutter. Following these filtering steps, vertical profiles of radar reflectivity are constructed to quantify migration activity from 100- to 3,000-m layer above ground level (AGL), from spring (1 March–15 June) 1995 to spring 2018. Some sites have data over a shorter period. To analyze the timing of migration, consistent with Horton et al. (2020), we used median migration date (q50), defined as the date by which 50% of the cumulative passage occurred at each radar station.

#### Weather and climate data

Monthly meteorological data are obtained from NASA Modern-Era Retrospective Analysis for Research and Applications, version 2 (MERRA-2, Gelaro et al. 2017). That includes upper-level geopotential heights and meridional (north—south) wind as well as 2-m air temperature (T-2m above the surface), available at  $0.5^{\circ} \times 0.625^{\circ}$  regular latitude—longitude grids.

We used the 300-hPa pressure level for geopotential heights and winds to capture the quasi-stationary Rossby waves, although similar wave patterns were also apparent at 500 hPa (Holton et al. 2003). These waves appear as a series of troughs and ridges looping around the globe with typical zonal wavenumbers of 4–6. Rossby waves, and in particular, tropically forced Rossby waves (Hoskins and Karoly 1981), play an important role in modulating midlatitude weather at subseasonal to seasonal time scales. Since these waves tend to be barotropic (do not vary in the vertical) in middle latitudes, their impacts extend down to the near-surface meteorological fields, including T-2m (e.g., Schubert et al. 2011), which we have used as a proxy for temperature variability within the layer that most of the migration occurs (up to ~1,500 m AGL). Pressure level corresponding to the top of this layer varies across CONUS due to the east–west topographic contrast. For this reason, we have verified for the western and eastern CONUS separately, that temperature patterns remain vertically uniform in the bird migration layer, so that we would be able to use T-2m to represent that layer.

For composite analysis—focusing on select extreme years—the meteorological variables were averaged over April and May to represent the peak cumulative flow of migratory birds. For correlation analysis, we used the entire spring migration season (March—May, MAM). A regional mean time series was generated for the western and eastern sectors of the United States, separated at 102°W longitude, using an objective regionalization approach discussed in the next section. Anomaly time series (subtracting the mean) were used for comparing the data that have the same unit such as in Fig. 1b. When data with different units were compared (such as in Fig. 3), each time series was standardized by subtracting the mean and dividing by the standard deviation. In either case the time series were linearly detrended to focus on

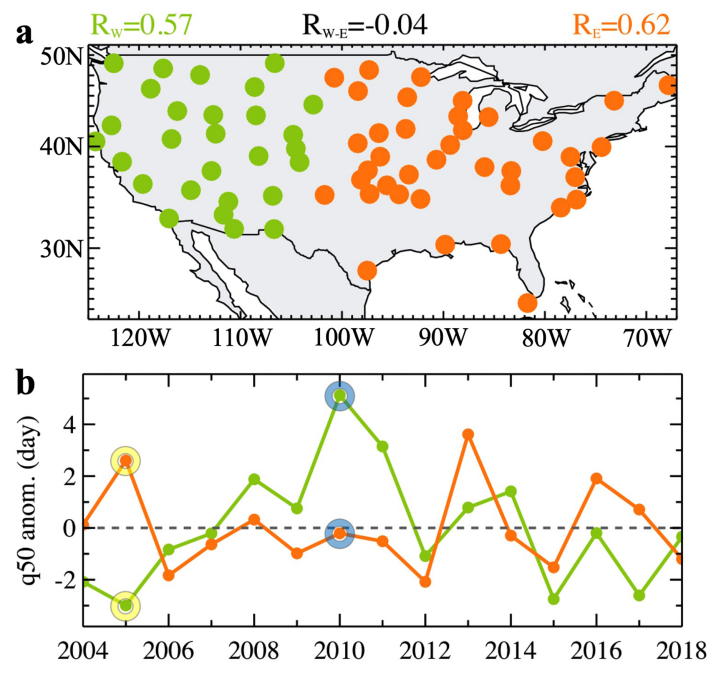


Fig. 1. (a) Two regions identified based on interannual variability of peak bird migration date (q50) in spring. Circles show the location of NEXRAD stations in each region. (b) Regional mean time series of the two regions. Time series are detrended anomalies. Years with notably west–east contrast in q50 anomalies are marked with open circles.

interannual variability. Note that because of sporadic data coverage in space and time, the time series are normalized (or standardized) based on the mean and standard deviation of the period on which they are presented, e.g., 2004–18 for Fig. 1b.

In addition to regional air temperature, seasonal time series of the normalized difference vegetation index (NDVI) and various climate indices were correlated with q50. The *p* value for each correlation coefficient was then adjusted using the false discovery rate method (Benjamini and Hochberg 1995). These indices that represent different modes of climate variability over the Pacific and Atlantic Oceans include Niño-3.4, Pacific–North American index

(PNA), east Pacific—North Pacific Oscillation (EP—NP), North Pacific pattern (NP), Pacific decadal oscillation (PDO), North Atlantic Oscillation (NAO), Arctic Oscillation (AO), North Tropical Atlantic index (NTA), and Atlantic Meridional Mode (AMM). The climate indices data were obtained from NOAA's Physical Science Laboratory (https://psl.noaa.gov/data/climateindices/list/). Monthly NDVI was used from the Moderate Resolution Imaging Spectroradiometer (MODIS) collection 6 product (MOD13C2), available at https://modis.gsfc.nasa.gov/data/dataprod/mod13.php.

#### Regionalization based on bird migration

Regionalization is a common practice for climate variability analysis (Fovell and Fovell 1993; Comrie and Glenn 1998; Dezfuli 2011; Dezfuli and Nicholson 2013). However, to the best of our knowledge, this is the first study to perform an objective regionalization based on interannual variability of bird migratory phenology at the continental scale. The process involved multiple steps and quality control measures to ensure the robustness of the spatiotemporal patterns and properly address the issues arising from the gaps and intrinsic noise in migratory data. Those efforts have resulted in excluding stations with a large number of missing data as well as those with noisy behavior that are most likely dominated by local characteristics.

In preparing the data, we first identified and at this initial stage eliminated the years in which more than half the stations had missing data. A second filter was applied to keep only stations that had q50 observations over all those years. These restricting criteria were imposed to meet the minimum requirements for a first estimate of regionalization and provided a 35 (stations)  $\times$  21 (years) matrix used in the regionalization model HiClimR (Badr et al. 2015). This is an open-source tool that uses hierarchical clustering to regionalize any number of spatial points such as radar stations into homogeneous regions with respect to similarity of their temporal variability. Note that the 21 years used in the initial stage may not necessarily represent a continuous period. This step of the analysis tried to maximize the number of years, so that the temporal similarity between stations would be meaningful.

It aimed to simultaneously maintain a minimum number of stations that would provide a reasonable representation of the spatial variability. This effort would inform us about the optimum number of regions and the longitudes at which they should be separated, therefore the  $35 \times 21$  matrix was not used to generate regional time series. The results at this stage are used as a guideline and suggested an optimum number of two regions, separated at about  $102^{\circ}$ W longitude. Using these two pieces of information, we modified the preliminary results in order to address the known intrinsic shortcoming of hierarchical algorithms that may result in removing or reassigning inconsistent members. In addition, applying those assumptions to the q50 data allowed for larger spatial coverage and maintained temporal continuity of the regional mean q50.

Consequently, 2004–18 was chosen as a period over which most stations (121 of 143) had continuous observations. Two regional time series were created, by averaging standardized q50 anomalies of all stations located to the west and east of  $102^{\circ}$ W, respectively. Pearson correlation coefficient between each regional time series and all its individual members were calculated. The stations with a correlation coefficient less than 0.4 (an arbitrary value corresponding to p < 0.14) were flagged as noise. Modified regional time series were calculated after removing those stations, so that they would represent the large-scale spatial signal in bird migration phenology. The regional time series were then detrended to focus on the interannual variability. The western and eastern regions consisted of 28 and 38 stations, respectively.

We evaluated the regionalization performance using intraregional and interregional correlations (Dezfuli 2011; Badr et al. 2015, 2016). A high value of "intraregional," defined as the mean correlation between each regional time series and its members, assures homogeneity of the regions. A low value of "interregional," defined as the correlation between regional mean time series, satisfies separability of the regions. Both these criteria were simultaneously met in our regionalization (Fig. 1a), as shown in the high intraregional correlations for western ( $R_W = 0.57$ ) and eastern ( $R_E = 0.62$ ) regions as well as in the low value for interregional correlation ( $R_{W-E} = -0.04$ ).

It is important to emphasize that we have used anomalies rather than absolute values of q50 because we are interested in regional interannual variability. Using anomalies would allow equal contribution from all stations to the regional means. Therefore, areal average time series would represent the entire region and are not biased toward stations with higher q50 values located in the northern latitudes. To further elaborate on this approach, we have compared two arbitrary stations in the western region (KMTX, 41.3°N, 112.4°W and KNKX, 32.9°N, 117°W). The correlation coefficient between their time series was 0.75 (p < 0.005), though they are ~1,000 km apart and the mean q50 of the northern stations is ~13 days higher. Similarly, the time series of KGRB (44.5°N, 88.1°W) and KTLH (30.4°N, 84.3°W) in the eastern region—nearly 1,600 km apart—are highly correlated (R = 0.78, p < 0.0001). It is interesting that some stations in the western region (e.g., KDAX, 38.5°N, 121.6°W) are strongly negatively correlated (R = -0.69, P < 0.005) with other stations in the eastern region such as KTLH, located ~3,500 km away. However, this dipole does not seem to be a continental-scale characteristic since  $R_{WF}$  is nearly zero and therefore is not further investigated in this study.

We also tried the regionalization for three and four regions, but both were rejected as the separability criterion was not achieved. At this stage the regionalization process is complete, and we next explored the differences between the temporal characteristics of the two regions such as their interannual variability. The standard deviation of regional mean time series of q50 anomalies over the period 2004-18 shows a relatively higher variability in the western region (2.4 days) than in its eastern counterpart (1.7 days). Using a two-tailed F test, the difference between variance of the two regional time series takes a P value less than 0.22.

Our two-region compartmentalization is intrinsically different from the previously used classifications, which are based on three- and four-flyway strategies, both in how it has been

achieved and its applications. Our approach reflects the interannual variability in timing of bird arrival and therefore is distinct from migratory corridors. We utilized an objective statistical approach to define the regions. This work relies on the fact that variability of bird migration phenology can be divided into two components, "noise" and "signal." The noise part may be determined by factors such as local environmental conditions, local geographical features, and species-specific characteristics (Vardanis et al. 2011; Somveille et al. 2019; Deppe et al. 2015; Youngflesh et al. 2021). On the other hand, common behavioral factors among species as well as large-scale climatic phenomena would collectively result in a spatiotemporal signal in interannual variability. We argue that our regionalization approach, reflecting this coherent "spatial signal," enables us to better identify the drivers of interannual and potentially decadal variability of migration timing at the continental scale. Here, we provide examples of large-scale impacts of climate conditions on bird migration, facilitated by our regionalization. It is worth noting that the 3-yr running averages are only used to qualitatively discuss the low-frequency variability in data. All quantitative analysis, including regionalization, significance tests, and correlations incorporate unsmoothed time series.

# Climate-migration association for the two regions

Comparing the mean time series of the two regions (Fig. 1b) allowed us to identify years with notably east—west contrast in median passage date anomalies. That contrast was most evident in 2005 and 2010, when the western and eastern sectors experienced considerably different median passage dates, with the western region exhibiting an earlier date in 2005 and a later date in 2010. We attribute this zonal (east—west) dipole pattern in q50, in part, to the near-surface air temperature (Fig. 2a) and, to a lesser degree, the meridional winds (Fig. 2b) during the peak migration months, April and May. The warmer than normal temperatures and southerly anomalies over the western region in 2005 favor an earlier arrival than in 2010. The opposite pattern is apparent for the eastern region. The strong linkage with temperature is likely due to the fact that temperature serves as a surrogate for resources

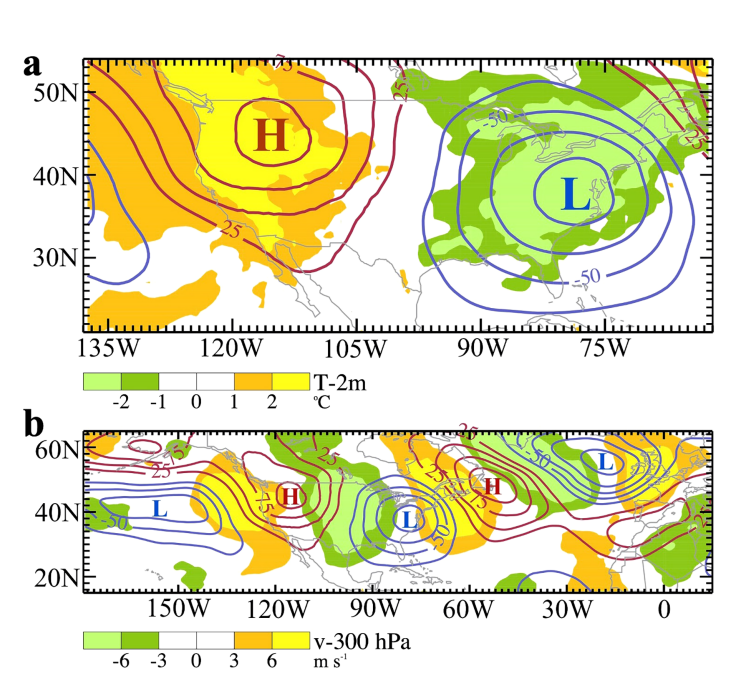


Fig. 2. (a) T-2m (shading) and geopotential heights at the 300-hPa level during April/May (blue and red contour lines) for 2005 minus 2010. (b) As in (a), but for 300-hPa meridional wind (shading) over a longitudinally extended area to capture the Rossby wave train. Regions with high and low pressure anomalies are labeled with H and L, respectively.

(Studds and Marra 2011; Van Doren and Horton 2018). We speculate that the winds at the height of migrating birds that are linked to the gradient of surface temperature via thermal wind balance may play a secondary role. This zonal configuration of temperature and meridional winds resembles a pattern that is consistent with that of a quasistationary atmospheric Rossby wave. The spatial structure of geopotential heights captures the areas of high- and low-pressure anomalies, associated with the wave (Fig. 2a). This anomaly pattern over the United States is part of a wave train that extends from the central North Pacific into the North Atlantic (Fig. 2b); it was especially prominent during 2010. The effect of the

Table 1. Pearson correlation coefficient between regional mean q50 and seasonal (MAM) mean of various climate indices. Calculations are made for both 2004–18 (n=15) with minimum missing data and the extended period 1996–2018 (n=23). Corresponding p values, adjusted with the false discovery rate method (Benjamini and Hochberg 1995) are also provided (in parentheses). Only adjusted p values close to or less than 0.1 are shown (in boldface).

Climate index	Region	2004–18	1996–2018
T-2m	West	-0.83 (0.0009)	-0.79 (0.000 05)
	East	-0.55 (0.08)	-0.56 (0.02)
NDVI	West	-0.63 (0.04)	-0.50 (0.1)*
	East	-0.17	-0.12
Niño-3.4	West	-0.33	-0.24
	East	0.28	0.30
EP/NP	West	-0.37	-0.17
	East	0.55 (0.08)	0.58 (0.02)
PDO	West	-0.35	-0.29
	East	0.31	0.42 (0.06)
AO	West	-0.02	0.00
	East	-0.60 (0.08)	-0.50 (0.03)
NTA	West	0.34	0.21
	East	0.49 (0.11)	0.52 (0.03)

\*For 2000-18.

waves—likely triggered by sea surface temperature (SST) anomalies over the Pacific Ocean—is reflected at the lower troposphere through downward penetration of potential vorticity.

Another capability of our regionalization approach is that it enables us to identify variability patterns specific to each region and their associated controlling factors. One advantage of objective regionalization is that once the borders are determined, the regions are assumed homogeneous and therefore the time series can be extended over the years that were excluded from the original regionalization due to the low number of sites with data available. This advantage allowed us to extend the time series of q50 over 1996-2018, recognizing the potential uncertainties and errors,

arising from using a smaller number of stations for the years prior to 2004. However, we have computed correlation coefficient between q50 and various climate indices for both periods (Table 1).

The western region shows a significant negative correlation with T-2m averaged over the same area (R = -0.79) for 1996–2018. One noticeable pattern in q50 of this region is its low-frequency variability that is also apparent in the regional T-2m (Fig. 3) and PDO (not shown), where positive and negative phases of PDO are coincident with early and late arrival dates, respectively. However, we recognize that the period of this analysis is not sufficiently long to confidently support this link, which can be considered as a viable hypothesis for further investigation when data become available. In contrast, a low-frequency pattern is not evident over the eastern region, and q50 over this area shows a weaker interannual association, though statistically significant, with its regional mean temperature

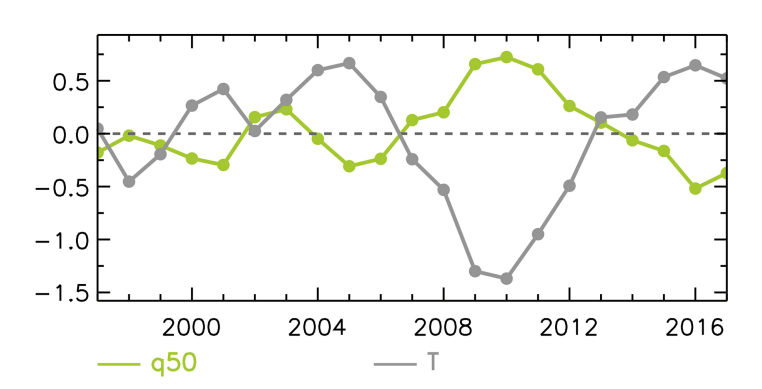


Fig. 3. The 3-yr running average of spring q50 and T-2m seasonal mean (MAM) over the western region. Time series are standardized and detrended for better comparison of variables with different units.

(*R* = −0.56). This different magnitude of response to temperature is intriguing because CONUS can be divided into two homogeneous regions with respect to interannual variability of spring temperature (MAM), and the separating longitude is roughly the same as that of the regions based on q50 (Fig. 4). The regionalization was objectively performed with HiClimR package, using seasonal T-2m gridded data from MERRA-2. The two-region

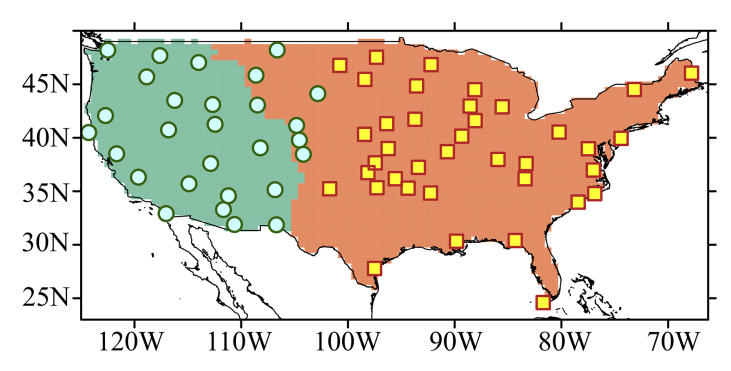


Fig. 4. Climate regions obtained objectively based on similarity in interannual variability of MAM T-2m (shading). Location of the stations for the two regions identified based on interannual variability of peak migration date (q50) are superimposed for comparison.

classification was obtained from simultaneous minimization of interregional and maximization of intraregional correlations. In addition, this division closely corresponds to differences in patterns of greenness and habitat between eastern and western CONUS (White et al. 2005). Interannual variability of q50 in the western region presents a strong negative correlation (R = -0.50) with NDVI—unlike the eastern region (R = -0.12,

Table 1). The latter low correlation may be attributed to several factors including heterogeneity of interannual variability of greenness within the eastern region and species and latitudinal dependencies on vegetation patterns (Mayor et al. 2017; Youngflesh et al. 2021).

Although the eastern region shows relatively weaker association with regional variability, its link to teleconnection patterns is stronger than that of the western region (Table 1). The highest correlations are with EP–NP (R=0.58), NTA (R=0.52), and AO (R=-0.50) indices. To assess the extent to which these climate phenomena manifest the impact of ocean variability on bird migration, we evaluated the spatial correlation between q50 of the eastern region and large-scale SSTs (Fig. 5a). The spatial patterns of EP–NP and NTA can be particularly identified from the regions with significant correlations, although the North Pacific correlations may also resemble the PDO structure. Analysis of spatial correlation between 300-hPa geopotential heights and q50 shows that the impact of SST is likely reflected through Rossby waves that are excited over the tropical Pacific (Fig. 5b). These waves are often associated with the North American ridge—trough dipole that controls the temperature over the eastern CONUS. Although the dipole is commonly known for its influ-

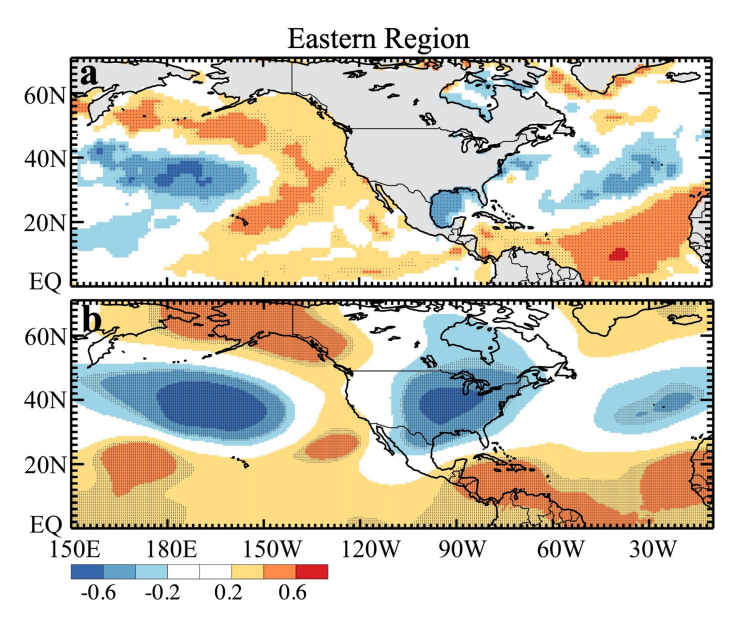


Fig. 5. Correlation patterns between regional q50 time series of the eastern region and the large-scale (a) SST and (b) 300-hPa geopotential heights. All time series are seasonal means (MAM) for 1996–2018. Black dots show areas with correlation coefficient significant at the 10% level.

ence on boreal winter temperature (Wang et al. 2014; Singh et al. 2016; Schulte et al. 2018), it is also present during spring (Schulte and Lee 2017).

The western region, on the other hand, shows strong correlation only with geopotential heights over the same area and SSTs along the west coast of North America (Fig. 6). The negative correlations with SST imply that the adjacent waters likely affect the region through temperature advection. A Rossby wave train originating from the tropical Pacific is also apparent (Fig. 6b), but it is much weaker and more spatially limited than the one shown for the eastern region. Additional climate modes

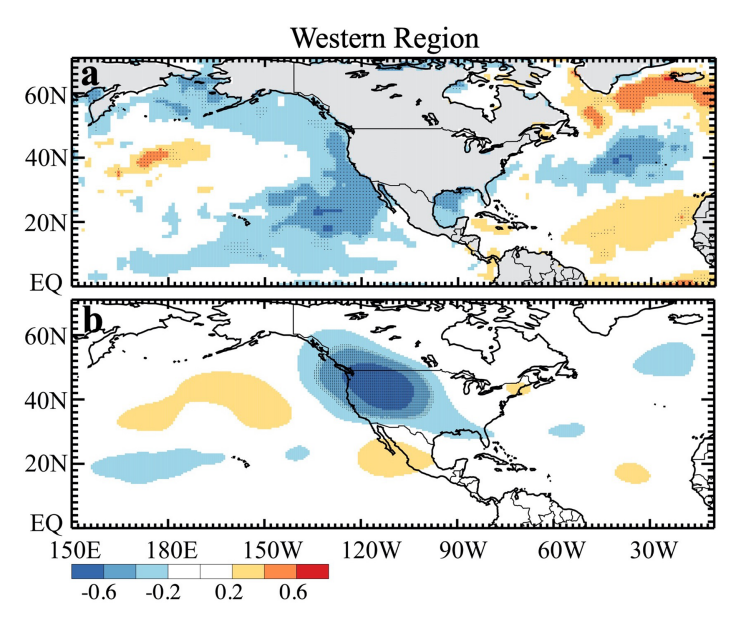


Fig. 6. As in Fig. 5, but for the western region.

were examined but the results were not included in Table 1 because they were either not statistically significant (e.g., PNA) or considered redundant due to high covariability with indices already presented in the table. For example, NTA was highly correlated with AMM (R = 0.9), so was AO with NAO (R = 0.74)and PDO with NP (R = -0.7). However, the climate modes shown in Table 1 would adequately represent variability over both tropical and extratropical parts of the Pacific and Atlantic Oceans.

# **Discussions and future work**

Our analysis approach is different from previous studies of long-term changes, which have largely focused on the trends of migration phenology; many do not consider year-to-year variability in these dynamics. In contrast, our approach has incorporated detrended data to facilitate the study of interannual variability and its drivers. As a by-product, this strategy detects the years during which the western and eastern United States present an opposite migratory behavior and attempts to explore climatic processes responsible for such a diploe pattern.

Some differences were noticed between drivers of interannual variability of the western and eastern regions. While the western region shows a strong link to the regional temperature, the eastern region presents statistically significant relationships with several climate modes of variability including atmospheric Rossby waves, which appear to be excited in the tropical Pacific Ocean. While some covariability may exist between these modes, some of them can act quite independently, suggesting that bird migration is likely controlled by combined effect of these teleconnections. Such complex interactions require further investigation. Also, we speculate that spatial variability of species composition may partly contribute to different responses of the western and eastern regions to regional climate conditions (La Sorte et al. 2014b; Horton et al. 2020). However, NEXRAD data are agnostic to species composition, therefore long-term species-specific observations with high spatial resolution, for example, from citizen science would be crucial to address this question. Other potential future work could focus on future projection of spring temperature variability mainly for the western region, changes in teleconnections affecting the eastern region, and seasonal prediction skill of atmospheric phenomena, such as Rossby waves, that influence the migration system. The new spatial framework presented here would facilitate such follow-up studies.

**Acknowledgments.** This study was supported by Global Modeling and Assimilation Office (GMAO) National Climate Assessment (NCA) enabling tools funded by NASA and the GMAO Core funding, provided under NASA's Modeling, Analysis and Prediction (MAP) program. Constructive comments from three reviewers substantially improved the manuscript. Valuable discussion with Prof. Peter Marra of Georgetown University is also appreciated. The authors would like to appreciate constructive discussions with members of the NCA group at GMAO. Kyle Horton's contributions were supported by

the National Science Foundation Macrosystems Biology and NEON-Enabled Science project 2017554. Benjamin Zuckerberg contribution was supported by the National Science Foundation Macrosystems Biology and NEON-Enabled Science project 1926428.

**Data availability statement.** The bird migration datasets are available at https://doi.org/10.6084/m9.figshare.10062239.v1. MERRA-2 products are publicly available at https://disc.gsfc.nasa.gov with https://doi.org/10.5067/KVIMOMCUO83U for T-2m and https://doi.org/10.5067/2E096JV59PK7 for upper levels. PDO time series can be found at http://research.jisao.washington.edu/pdo/PDO.latest.

# References

- Alerstam, T., A. Hedenström, and S. Åkesson, 2003: Long-distance migration: Evolution and determinants. *Oikos*, **103**, 247–260, https://doi.org/10.1034/j.1600-0706.2003.12559.x.
- Ansari, S., and Coauthors, 2018: Unlocking the potential of NEXRAD data through NOAA's Big Data Partnership. *Bull. Amer. Meteor. Soc.*, 99, 189–204, https://doi.org/10.1175/BAMS-D-16-0021.1.
- Badr, H. S., B. F. Zaitchik, and A. K. Dezfuli, 2015: A tool for hierarchical climate regionalization. *Earth Sci. Inf.*, 8, 949–958, https://doi.org/10.1007/s12145-015-0221-7.
- —, A. K. Dezfuli, B. F. Zaitchik, and C. D. Peters-Lidard, 2016: Regionalizing Africa: Patterns of precipitation variability in observations and global climate models. J. Climate, 29, 9027–9043, https://doi.org/10.1175/JCLI-D-16-0182.1.
- Ballard, G., G. R. Geupel, N. Nur, and T. Gardali, 2003: Long-term declines and decadal patterns in population trends of songbirds in western North America, 1979–1999. Condor, 105, 737–755, https://doi.org/10.1093/condor/105.4.737.
- Benjamini, Y., and Y. Hochberg, 1995: Controlling the false discovery rate: A practical and powerful approach to multiple testing. *J. Roy. Stat. Soc.*, **57B**, 289–300, https://doi.org/10.1111/j.2517-6161.1995.tb02031.x.
- Cohen, E. B., F. R. Moore, and R. A. Fischer, 2012: Experimental evidence for the interplay of exogenous and endogenous factors on the movement ecology of a migrating songbird. *PLOS ONE*, 7, e41818, https://doi.org/10.1371/journal. pone.0041818.
- Comrie, A. C., and E. C. Glenn, 1998: Principal components-based regionalization of precipitation regimes across the southwest United States and northern Mexico, with an application to monsoon precipitation variability. *Climate Res.*, **10**, 201–215, https://doi.org/10.3354/cr010201.
- Deppe, J. L., and Coauthors, 2015: Fat, weather, and date affect migratory songbirds' departure decisions, routes, and time it takes to cross the Gulf of Mexico. Proc. Natl. Acad. Sci. USA, 112, E6331–E6338, https://doi.org/10.1073/pnas.1503381112.
- Dezfuli, A. K., 2011: Spatio-temporal variability of seasonal rainfall in western equatorial Africa. *Theor. Appl. Climatol.*, **104**, 57–69, https://doi.org/10.1007/s00704-010-0321-8.
- —, and S. E. Nicholson, 2013: The relationship of rainfall variability in western equatorial Africa to the tropical oceans and atmospheric circulation. Part II: The boreal autumn. *J. Climate*, 26, 66–84, https://doi.org/10.1175/JCLI-D-11-00686.1.
- Dokter, A. M., and Coauthors, 2018: Seasonal abundance and survival of North America's migratory avifauna determined by weather radar. *Nat. Ecol. Evol.*, **2**, 1603–1609, https://doi.org/10.1038/s41559-018-0666-4.
- —, and Coauthors, 2019: bioRad: Biological analysis and visualization of weather radar data. *Ecography*, 42, 852–860, https://doi.org/10.1111/ecog.04028.
- Fovell, R. G., and M. Y. C. Fovell, 1993: Climate zones of the conterminous United States defined using cluster analysis. *J. Climate*, **6**, 2103–2135, https://doi.org/10.1175/1520-0442(1993)006<2103:CZOTCU>2.0.CO;2.
- Gauthreaux, S. A., 1971: A radar and direct visual study of passerine spring migration in southern Louisiana. *The Auk*, **88**, 343–365, https://doi.org/10.2307/4083884.
- Gelaro, R., and Coauthors, 2017: The Modern-Era Retrospective Analysis for Research and Applications, version 2 (MERRA-2). *J. Climate*, **30**, 5419–5454, https://doi.org/10.1175/JCLI-D-16-0758.1.
- Gordo, O., 2007: Why are bird migration dates shifting? A review of weather and climate effects on avian migratory phenology. *Climate Res.*, 35, 37–58, https://doi.org/10.3354/cr00713.
- Gwinner, E., 1996: Circadian and circannual programmes in avian migration. J. Exp. Biol., 199, 39–48, https://doi.org/10.1242/jeb.199.1.39.
- Hawkins, A. S., 1984: *Flyways: Pioneering Waterfowl Management in North America*. Fish and Wildlife Service, U.S. Department of the Interior, 517 pp.
- Holton, J. R., J. A. Curry, and J. A. Pyle, 2003: Encyclopedia of Atmospheric Sciences. Academic Press, 2780 pp.
- Horton, K. G., and Coauthors, 2020: Phenology of nocturnal avian migration has shifted at the continental scale. *Nat. Climate Change*, **10**, 63–68, https://doi. org/10.1038/s41558-019-0648-9.

- Hoskins, B. J., and D. J. Karoly, 1981: The steady linear response of a spherical atmosphere to thermal and orographic forcing. *J. Atmos. Sci.*, **38**, 1179–1196, https://doi.org/10.1175/1520-0469(1981)038<1179:TSLROA>2.0.CO;2.
- La Sorte, F. A., D. Fink, W. M. Hochachka, J. P. DeLong, and S. Kelling, 2014a: Spring phenology of ecological productivity contributes to the use of looped migration strategies by birds. *Proc. Roy. Soc.*, 281B, 20140984, https://doi. org/10.1098/rspb.2014.0984.
- —, and Coauthors, 2014b: The role of atmospheric conditions in the seasonal dynamics of North American migration flyways. *J. Biogeogr.*, **41**, 1685–1696, https://doi.org/10.1111/jbi.12328.
- Lane, J. E., L. E. Kruuk, A. Charmantier, J. O. Murie, and F. S. Dobson, 2012: Delayed phenology and reduced fitness associated with climate change in a wild hibernator. *Nature*, 489, 554–557, https://doi.org/10.1038/nature11335.
- Lin, T. Y., and Coauthors, 2019: MistNet: Measuring historical bird migration in the US using archived weather radar data and convolutional neural networks. *Methods Ecol. Evol.*, 10, 1908–1922, https://doi.org/10.1111/2041-210X.13280.
- Lincoln, F. C., 1935: The waterfowl flyways of North America. Circular 342, U.S. Department of Agriculture, 13 pp.
- Lowery, G. H., Jr., 1945: Trans-Gulf spring migration of birds and the coastal hiatus. *Wilson Bull.*, **57**, 92–121.
- Mayor, S. J., and Coauthors, 2017: Increasing phenological asynchrony between spring green-up and arrival of migratory birds. *Sci. Rep.*, **7**, 1902, https://doi.org/10.1038/s41598-017-02045-z.
- Oliver, R. Y., P. J. Mahoney, E. Gurarie, N. Krikun, B. C. Weeks, M. Hebblewhite, G. Liston, and N. Boelman, 2020: Behavioral responses to spring snow conditions contribute to long-term shift in migration phenology in American robins. *Environ. Res. Lett.*, 15, 045003, https://doi.org/10.1088/1748-9326/ab71a0.
- Olsen, B., Munster, V. J., Wallensten, A., Waldenström, J., Osterhaus, A. D. and Fouchier, R. A., 2006: Global patterns of influenza A virus in wild birds. Science, 312, 384–388, https://doi.org/10.1126/science.1122438.
- Rosenberg, K. V., and Coauthors, 2019: Decline of the North American avifauna. *Science*, **366**, 120–124, https://doi.org/10.1126/science.aaw1313.
- Schubert, S., H. Wang, and M. Suarez, 2011: Warm season subseasonal variability and climate extremes in the Northern Hemisphere: The role of stationary Rossby waves. J. Climate, 24, 4773–4792, https://doi.org/10.1175/JCLI-D-10-05035.1.
- Schulte, J. A., and S. Lee, 2017: Strengthening North Pacific influences on United States temperature variability. *Sci. Rep.*, **7**, 124, https://doi.org/10.1038/s41598-017-00175-y.
- ——, N. Georgas, V. Saba, and P. Howell, 2018: North Pacific influences on long island sound temperature variability. *J. Climate*, 31, 2745–2769, https://doi.org/10.1175/JCLI-D-17-0135.1.
- Singh, D., D. L. Swain, J. S. Mankin, D. E. Horton, L. N. Thomas, B. Rajaratnam, and N. S. Diffenbaugh, 2016: Recent amplification of the North American winter temperature dipole. *J. Geophys. Res. Atmos.*, 121, 9911–9928, https://doi. org/10.1002/2016JD025116.
- Smith, J. A., and J. L. Deppe, 2008: Simulating the effects of wetland loss and inter-annual variability on the fitness of migratory bird species. 2008 IEEE Int. Geoscience and Remote Sensing Symp., Boston, MA, IEEE, IV-838–IV-841, https://doi.org/10.1109/IGARSS.2008.4779853.
- Somveille, M., A. Manica, and A. S. Rodrigues, 2019: Where the wild birds go: Explaining the differences in migratory destinations across terrestrial bird species. *Ecography*, **42**, 225–236, https://doi.org/10.1111/ecog.03531.
- Strong, C., B. Zuckerberg, J. L. Betancourt, and W. D. Koenig, 2015: Climatic dipoles drive two principal modes of North American boreal bird irruption. *Proc. Natl. Acad. Sci. USA*, 112, E2795–E2802, https://doi.org/10.1073/pnas.1418414112.
- Studds, C. E., and P. P. Marra, 2011: Rainfall-induced changes in food availability modify the spring departure programme of a migratory bird. *Proc. Roy. Soc.*, 278B, 3437–3443, https://doi.org/10.1098/rspb.2011.0332.

- Van Buskirk, J., R. S. Mulvihill, and R. C. Leberman, 2009: Variable shifts in spring and autumn migration phenology in North American songbirds associated with climate change. *Global Change Biol.*, **15**, 760–771, https://doi.org/10.1111/j.1365-2486.2008.01751.x.
- Van Doren, B. M., and K. G. Horton, 2018: A continental system for forecasting bird migration. *Science*, 361, 1115–1118, https://doi.org/10.1126/science. aat7526.
- Vardanis, Y., R. H. Klaassen, R. Strandberg, and T. Alerstam, 2011: Individuality in bird migration: Routes and timing. *Biol. Lett.*, 7, 502–505, https://doi.org/10.1098/rsbl.2010.1180.
- Waller, E. K., T. M. Crimmins, J. J. Walker, E. E. Posthumus, and J. F. Weltzin, 2018: Differential changes in the onset of spring across US National Wildlife Refuges and North American migratory bird flyways. *PLOS ONE*, 13, e0202495, https://doi.org/10.1371/journal.pone.0202495.
- Wang, S. Y., L. Hipps, R. R. Gillies, and J. H. Yoon, 2014: Probable causes of the abnormal ridge accompanying the 2013–2014 California drought: ENSO precursor and anthropogenic warming footprint. *Geophys. Res. Lett.*, **41**, 3220–3226, https://doi.org/10.1002/2014GL059748.
- White, A. B., P. Kumar, and D. Tcheng, 2005: A data mining approach for understanding topographic control on climate-induced inter-annual vegetation variability over the United States. *Remote Sens. Environ.*, **98**, 1–20, https://doi.org/10.1016/j.rse.2005.05.017.
- Youngflesh, C., and Coauthors, 2021: Migratory strategy drives species-level variation in bird sensitivity to vegetation green-up. *Nat. Ecol. Evol.*, **5**, 987–994, https://doi.org/10.1038/s41559-021-01442-y.
- Zuckerberg, B., C. Strong, J. M. LaMontagne, S. S. George, J. L. Betancourt, and W. D. Koenig, 2020: Climate dipoles as continental drivers of plant and animal populations. *Trends Ecol. Evol.*, 35, 440–453, https://doi.org/10.1016/j.tree.2020.01.010.